Model Predictive Control of Axial Dispersion Tubular Reactors with Recycle: Addressing State-delay through Transport PDEs

Behrad Moadeli and Stevan Dubljevic[1]

***Abstract*— This paper presents the model predictive control of an axial tubular reactor with a recycle stream, where the intrinsic time delay imposed by the recycle stream—often overlooked in chemical engineering process control studies—is modeled as a transport PDE. This leads to a boundary-controlled system of coupled parabolic and hyperbolic PDEs under Danckwerts boundary conditions, specific for this reactor type. A discrete-time linear model predictive controller is designed to stabilize the system. Utilizing Cayley-Tustin time discretization along with the late lumping approach, the system's infinite-dimensional characteristics are preserved with no need for model reduction or spatial approximation. Numerical simulations demonstrate the controller's effectiveness in stabilizing an unstable system while satisfying input constraints.**

I. Introduction

Many chemical and petrochemical processes, such as reactions in reactors, heat transfer in exchangers, and separations in columns, involve states distributed in space and time. These systems, known as distributed parameter systems (DPS), are often modeled using partial differential equations (PDEs) to describe distributed state dynamics. Due to their infinite-dimensional nature, the control and estimation of DPSs are inherently more challenging compared to the well-established control theories for finite-dimensional systems [1], making this field an active area of research. Two primary methods, "Early Lumping" and "Late Lumping," have been proposed to address DPS control in the literature. The first, "Early Lumping," reduces the infinite-dimensional system to a finite-dimensional one through spatial discretization during the modeling phase [2]. While this enables standard control strategies, it often compromises model accuracy due to mismatches between the original and reduced-order systems [3]. In contrast, "Late Lumping" preserves the infinite-dimensional system until the final numerical implementation stage, resulting in more accurate but computationally complex control strategies.

Numerous studies have employed Late Lumping approaches to control infinite-dimensional systems in chemical engineering. These efforts primarily focus on convection-reaction systems governed by first-order hyperbolic PDEs and diffusion-convection-reaction systems governed by second-order parabolic PDEs. For example, robust control of first-order hyperbolic PDEs was explored in [4], where a plug flow reactor system was stabilized under distributed input. Similarly, boundary feedback stabilization using the backstepping method was proposed in [5] for such systems. State feedback regulator design for a countercurrent heat exchanger, another example of a chemical engineering DPS, was addressed in [6]. Introducing the effects of dispersion in axial dispersion tubular reactors, robust control of second-order parabolic PDEs was studied in [7]. Modal decomposition methods for designing low-dimensional predictive controllers for diffusion-convection-reaction systems have also been applied in [8], while observer-based model predictive control (MPC) was developed in [9] for axial dispersion tubular reactors, considering recycle stream effects.

Delay systems represent another class of infinite-dimensional systems studied extensively [10]. Commonly modeled using delay differential equations (DDEs), delays can alternatively be described using transport PDEs, offering advantages in complex scenarios [11]. In chemical engineering DPS control, input/output delays have been widely addressed, as industrial processes often feature both measurement and actuation delays. Such delays are typically handled by modeling them as transportation lag blocks, resulting in cascade PDE systems [12]–[14]. State delays, though less common, have been investigated in specific applications, such as heat exchangers with stream delays between passes [15], and plug flow tubular reactors with recycle delays [16], though none of these cases address the effects of diffusion. Even in works like [9], where recycle streams are considered for an axial dispersion tubular reactor, the recycle is assumed to be instantaneous, leaving a gap in the literature regarding state delays in diffusion-convection-reaction systems with recycle streams.

In this work, an axial dispersion reactor with recycle is modeled as a diffusion-convection-reaction DPS. The reactor dynamics are described by a second-order parabolic PDE, coupled with a first-order hyperbolic transport PDE to account for the recycle stream's state delay. A Late Lumping approach is employed, obtaining the system's resolvent in a closed operator form without spatial discretization. To implement MPC as a digital controller, the system is discretized using the Cayley-Tustin method, a Crank-Nicolson-type discretization that conserves the continuous system's characteristics, avoiding the need for model reduction. Numerical simulations demonstrate that the proposed controller stabilizes an unstable system optimally under input constraints.

[1]Behrad Moadeli and Stevan Dubljevic are with the Department of Chemical and Materials Engineering, University of Alberta, Edmonton, AB, Canada T6G 1H9 moadeli@ualberta.ca, stevan.dubljevic@ualberta.ca

Funding provided by the Natural Sciences and Engineering Research Council of Canada—NSERC (RGPIN-2022-03486).

II. Methodology

A. Model representation

The chemical process depicted in Fig. 1 illustrates a chemical reaction within an axial dispersion tubular reactor [17] where reactant A is converted into products. The reactor features a recycle mechanism, allowing a portion of the product stream to re-enter the reactor, ensuring the consumption of any unreacted substrate. The dynamics of the reactant concentration can be described by the second-order parabolic PDE given by (1)

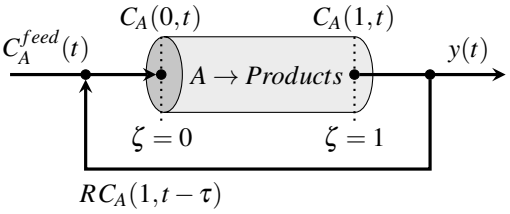

Fig. 1. Axial tubular reactor with recycle stream.

$$\dot{C}_A(\zeta,t) = D\partial_{\zeta\zeta}C_A(\zeta,t) - v\partial_\zeta C_A(\zeta,t) + r(C_A) \tag{1}$$

Here, $C_A(\zeta,t)$ is the concentration of reactant A along the reactor. The physical parameters D and v represent the diffusion coefficient and flow velocity along the reactor, respectively. Physical parameters are assumed to be constant, hence changes in temperature or pressure will not affect the reactor model. The coordinate system in space and time is represented by ζ and t, where $\zeta \in [0,1]$ and $t \in [0,\infty)$. In addition, $r(C_A)$ is the reaction rate of the reactant in general, which is often a non-linear function of C_A. Therefore, the model is further linearized around its steady-state, followed by introducing the deviation variable $c(\zeta,t) = C_A(\zeta,t) - C_{A,ss}(\zeta)$, where $C_{A,ss}(\zeta)$ is the steady-state concentration of the reactant. The linearized model is then given by (2).

$$\dot{c}(\zeta,t) = D\partial_{\zeta\zeta}c(\zeta,t) - v\partial_\zeta c(\zeta,t) + k_r c(\zeta,t) \tag{2}$$

Here, $k_r \equiv \left.\dfrac{\partial r(C_A)}{\partial C_A}\right|_{C_{A,ss}}$ is the linearized reaction rate coefficient in the vicinity of the steady-state. The system input is also defined as a deviation variable $u(t) \equiv C_A^{feed} - C_{A,ss}^{feed}$, representing the deviation of the concentration of the reactant being fed into the reactor from its steady-state value. The input stream is then mixed with the delayed state resulting from the recycled portion of the reactant at the reactor outlet occurring τ seconds back in time, forming one of the boundary conditions. In an attempt to make the model more realistic for common axial dispersion tubular reactors in chemical industry, Dankwerts boundary conditions are chosen as they are known to be suitable for this purpose by accounting for deviations from perfect mixing and piston flow, assuming negligible transport lags in connecting lines [18]. The boundary conditions are all represented in (3),

$$\begin{cases} D\partial_\zeta c(0,t) - vc(0,t) = -v\left[Rc(1,t-\tau) + (1-R)u(t)\right] \\ \partial_\zeta c(1,t) = 0 \\ y(t) = c(1,t) \end{cases} \tag{3}$$

where parameters R and τ represent the recycle ratio and the residence time along the recycle stream.

In the case where the problem involves similar forms of PDEs, an effective general practice to address delays in systems is to reformulate the problem such that the notion of delay is replaced with an alternative transport PDE. Therefore, a new state variable $\underline{x}(\zeta,t) \equiv [x_1(\zeta,t), x_2(\zeta,t)]^T$ is defined as a vector of functions, where $x_1(\zeta,t)$ represents the concentration within the reactor—analogous to $c(\zeta,t)$—and $x_2(\zeta,t)$ is introduced as a new state variable to account for the concentration along the recycle stream. The delay is thus modeled as a pure transport process, wherein the first state $x_1(\zeta,t)$ is transported from the reactor outlet to the inlet, experiencing a delay of τ time units while in the recycle stream. This makes all state variables expressed explicitly at a specific time instance t, resulting in the standard state-space form for a given infinite-dimensional linear time-invariant (LTI) system $\dot{\underline{x}} = \mathfrak{A}\underline{x} + \mathfrak{B}u$. Here, $\mathfrak{A}$ is a linear operator $\mathscr{L}(X)$ acting on a Hilbert space $X : L^2[0,1] \times L^2[0,1]$ as shown in (4). Also, $\mathfrak{B}$ is a linear operator that maps the scalar input from input-space onto the state space, as defined in (5).

$$\begin{aligned} \mathfrak{A} &\equiv \begin{bmatrix} D\partial_{\zeta\zeta} - v\partial_\zeta + k_r & 0 \\ 0 & \frac{1}{\tau}\partial_\zeta \end{bmatrix} \\ D(\mathfrak{A}) &= \Big\{ \underline{x}(\zeta) = [x_1(\zeta), x_2(\zeta)]^T \in X : \\ &\quad \underline{x}(\zeta), \partial_\zeta \underline{x}(\zeta), \partial_{\zeta\zeta}\underline{x}(\zeta) \quad \text{a.c.}, \\ &\quad D\partial_\zeta x_1(0) - vx_1(0) = -vRx_2(0), \\ &\quad \partial_\zeta x_1(1) = 0, x_1(1) = x_2(1) \Big\} \end{aligned} \tag{4}$$

$$\begin{aligned} \mathfrak{B} &\equiv \begin{bmatrix} \delta(\zeta) \\ 0 \end{bmatrix} v(1-R) \\ D(\mathfrak{B}) &= \Big\{ u \in \mathbb{R} \Big\} \end{aligned} \tag{5}$$

where $\delta(\zeta)$ is dirac delta function. This will enable the derivation of the system's spectrum using the eigenvalue problem. The characteristics equation of the system is obtained by solving the equation $det(\mathfrak{A} - \lambda_i\, I) = 0$ for λ_i, where $\lambda_i \in \mathbb{C}$ is the i^{th} eigenvalue of the system and I is the identity operator. Attempts to analytically solve this equation have failed; therefore, it is solved numerically using the parameters in Table I. These parameters are carefully chosen to reflect key characteristics of the system, i.e. diffusion, convection, reaction, and delayed recycle. A negative reaction coefficient (k_r) is used to induce instability for analysis, a condition uncommon for isothermal reactors but possible in specific cases like autocatalytic or inhibitory reactions. Figure 2 depicts the resulting eigenvalue distribution in the complex plane, confirming instability of the linearized model near its steady state.

Attempts to analytically solve this equation has failed; therefore, it is solved numerically using the parameters in Table I. The resulting eigenvalue distribution is depicted in Figure 2 in the complex plane.

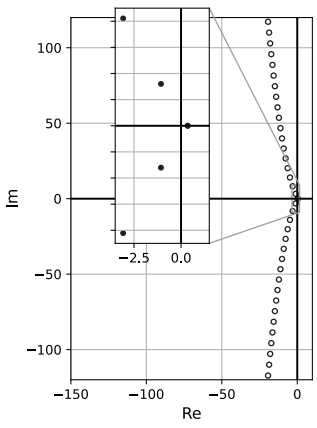

Fig. 2. Eigenvalues of operator $\mathfrak{A}$.

TABLE I
PHYSICAL PARAMETERS FOR THE SYSTEM

Parameter	Symbol	Value	Unit
Diffusivity	D	2×10^{-5}	m^2/s
Velocity	v	0.01	m/s
Reaction Constant	k_r	-1.5	s^{-1}
Recycle Residence Time	τ	80	s
Recycle Ratio	R	0.3	–

B. Adjoint system

Next step is to obtain the adjoint system operators $\mathfrak{A}^*$ and $\mathfrak{B}^*$. Utilizing the relation $\langle \mathfrak{A}\underline{x}+\mathfrak{B}u,\underline{y}\rangle = \langle \underline{x},\mathfrak{A}^*\underline{y}\rangle + \langle u,\mathfrak{B}^*\underline{y}\rangle$, the adjoint operators $\mathfrak{A}^*$ and $\mathfrak{B}^*$ are obtained as shown in (6) and (7), respectively.

$$\begin{aligned}
\mathfrak{A}^* &= \begin{bmatrix} D\partial_{\zeta\zeta}+v\partial_\zeta+k_r & 0 \\ 0 & -\frac{1}{\tau}\partial_\zeta \end{bmatrix} \\
D(\mathfrak{A}^*) &= \Big\{ \underline{y}=[y_1,y_2]^T \in Y : \\
&\qquad \underline{y}(\zeta),\partial_\zeta\underline{y}(\zeta),\partial_{\zeta\zeta}\underline{y}(\zeta) \quad \text{a.c.}, \\
&\qquad D\partial_\zeta y_1(1)+vy_1(1)=\frac{1}{\tau}y_2(1), \\
&\qquad Rvy_1(0)=\frac{1}{\tau}y_2(0), \partial_\zeta y_1(0)=0 \Big\}
\end{aligned} \tag{6}$$

$$\mathfrak{B}^*(\cdot) = \left[v(1-R)\int_0^1 \delta(\zeta)(\cdot)d\zeta \quad , \quad 0 \right] \tag{7}$$

Once the adjoint operators are determined, the eigenfunctions $\{\underline{\phi_i}(\zeta),\underline{\psi_i}(\zeta)\}$ (for $\mathfrak{A}$ and $\mathfrak{A}^*$, respectively) may be obtained and properly scaled following the calculation of eigenvalues. The set of scaled eigenfunctions will then form a bi-orthonormal basis for the Hilbert space X; which will be later used in the controller design. It is important to note that the system is not self adjoint, as the obtained adjoint operator and its domain are not the same as the original operator and its domain.

C. Resolvent operator

One must obtain the resolvent operator of the system $\mathfrak{R}(s,\mathfrak{A})=(sI-\mathfrak{A})^{-1}$ prior to constructing the discrete-time representation of the system. One way to obtain it is by utilizing the modal characteristics of the system, resulting in an infinite-sum representation of the operator. While being a common practice in the literature, truncating the infinite-sum representation for numerical implementation may lead to a loss of accuracy. Another way to express the resolvent operator is by treating it as an operator that maps either the initial condition of the system $\underline{x}(\zeta,0)$ or the input $u(t)$, to the Laplace transform of the state of the system $\underline{X}(\zeta,s)$. This approach, although more computationally intensive, results in a closed form expression for the resolvent operator, preserving the infinite-dimensional nature of the system. In (8), Laplace transform is applied to the LTI representation of the system for both zero-input response and zero-state response to obtain a general expression for the resolvent operator.

$$\begin{aligned}
&\dot{\underline{x}}(\zeta,t)=\mathfrak{A}\underline{x}(\zeta,t)+\mathfrak{B}u(t) \xrightarrow{\mathscr{L}} \\
&s\underline{X}(\zeta,s)-\underline{x}(\zeta,0)=\mathfrak{A}\underline{X}(\zeta,s)+\mathfrak{B}U(s) \\
&\begin{cases} \xrightarrow{u=0} & \underline{X}(\zeta,s)=(sI-\mathfrak{A})^{-1}\underline{x}(\zeta,0)=\mathfrak{R}(s,\mathfrak{A})\underline{x}(\zeta,0) \\ \xrightarrow{\underline{x}(0,\zeta)} & \underline{X}(\zeta,s)=(sI-\mathfrak{A})^{-1}\mathfrak{B}U(s)=\mathfrak{R}(s,\mathfrak{A})\mathfrak{B}U(s) \end{cases}
\end{aligned} \tag{8}$$

The goal is to obtain the solution for $\underline{X}(\zeta,s)$ and compare it with the general expression obtained in (8) to get the closed form expression for the resolvent operator. First step is to apply Laplace transform to the original system of PDEs in (4). The second order derivative term is decomposed to two first order PDEs, constructing a new 3×3 system of first order ODEs with respect to ζ after Laplace transformation, as shown in (9).

$$\begin{aligned}
\partial_\zeta \overbrace{\begin{bmatrix} X_1(\zeta,s) \\ \partial_\zeta X_1(\zeta,s) \\ X_2(\zeta,s) \end{bmatrix}}^{\tilde{\underline{X}}(\zeta,s)} &= \overbrace{\begin{bmatrix} 0 & 1 & 0 \\ \frac{s-k}{D} & \frac{v}{D} & 0 \\ 0 & 0 & s\tau \end{bmatrix}}^{P(s)} \begin{bmatrix} X_1(\zeta,s) \\ \partial_\zeta X_1(\zeta,s) \\ X_2(\zeta,s) \end{bmatrix} \\
&\quad + \underbrace{\begin{bmatrix} 0 \\ -\frac{x_1(\zeta,0)}{D}+v(1-R)\delta(\zeta)U(s) \\ -\tau x_2(\zeta,0) \end{bmatrix}}_{Z(\zeta,s)} \\
\Rightarrow \partial_\zeta\tilde{\underline{X}}(\zeta,s) &= P(s)\tilde{\underline{X}}(\zeta,s)+Z(\zeta,s)
\end{aligned} \tag{9}$$

with solution given by (10).

$$\tilde{\underline{X}}(\zeta,s)=\underbrace{e^{P(s)\zeta}}_{T(\zeta,s)}\tilde{\underline{X}}(0,s)+\int_0^\zeta \underbrace{e^{P(s)(\zeta-\eta)}}_{F(\zeta,\eta)}Z(\eta,s)d\eta \tag{10}$$

Since the boundary conditions are not homogeneous, $\tilde{\underline{X}}(0,s)$ needs to be obtained by solving the system of

algebraic equations given in (11); which is the result of applying Danckwerts boundary conditions to the Laplace transformed system of PDEs at $\zeta = 1$.

$$\begin{aligned}
&\overbrace{\begin{bmatrix} -v & D & Rv \\ T_{11}(1,s) & T_{12}(1,s) & -T_{33}(1,s) \\ T_{21}(1,s) & T_{22}(1,s) & 0 \end{bmatrix}}^{M^{-1}(s)} \underline{\tilde{X}}(0,s) = \\
&\underbrace{\int_0^1 \begin{bmatrix} 0 \\ F_{33}(1,\eta)Z_3(\eta,s) - F_{12}(1,\eta)Z_2(\eta,s) \\ -F_{22}(1,\eta)Z_2(\eta,s) \end{bmatrix} d\eta}_{\underline{b}(s)} \\
&\Rightarrow \underline{\tilde{X}}(0,s) = M(s)\underline{b}(s)
\end{aligned} \tag{11}$$

Having access to $\underline{\tilde{X}}(0,s)$, the solution for $\underline{X}(\zeta,s)$ can be explicitly derived. The resolvent operator for zero-input and zero-state cases are therefore obtained in a closed form as shown in (12) and (13), respectively.

$$\begin{aligned}
&U(s) = 0 \Rightarrow \mathfrak{R}(s,\mathfrak{A})\underline{(\cdot)} = \begin{bmatrix} \mathfrak{R}_{11} & \mathfrak{R}_{12} \\ \mathfrak{R}_{21} & \mathfrak{R}_{22} \end{bmatrix} \begin{bmatrix} (\cdot)_1 \\ (\cdot)_2 \end{bmatrix} \Rightarrow \\
&\mathfrak{R}_{11} = \sum_{j=1}^{2} \frac{T_{1j}(\zeta)}{D} \int_0^1 \left[M_{j2}F_{12}(1,\eta) + M_{j3}F_{22}(1,\eta) \right] (\cdot)_1 d\eta \\
&\qquad - \frac{1}{D} \int_0^\zeta F_{12}(\zeta,\eta)(\cdot)_1 d\eta \\
&\mathfrak{R}_{12} = \sum_{j=1}^{2} -\tau T_{1j}(\zeta) \int_0^1 M_{j2}F_{33}(1,\eta)(\cdot)_2 d\eta \\
&\mathfrak{R}_{21} = \frac{T_{33}(\zeta)}{D} \int_0^1 \left[M_{32}F_{12}(1,\eta) + M_{33}F_{22}(1,\eta) \right] (\cdot)_1 d\eta \\
&\mathfrak{R}_{22} = -\tau T_{33}(\zeta) \int_0^1 M_{32}F_{33}(1,\eta)(\cdot)_2 d\eta \\
&\qquad - \tau \int_0^\zeta F_{33}(\zeta,\eta)(\cdot)_2 d\eta
\end{aligned} \tag{12}$$

$$\begin{aligned}
&\underline{x}(\zeta,0) = 0 \Rightarrow \mathfrak{R}(s,\mathfrak{A})\mathfrak{B}(\cdot) = \begin{bmatrix} \mathfrak{R}_1\mathfrak{B} \\ \mathfrak{R}_2\mathfrak{B} \end{bmatrix} (\cdot) \Rightarrow \\
&\mathfrak{R}_1\mathfrak{B} = -v(1-R)\big[\sum_{j=1}^{2} T_{1j}(\zeta)(M_{j2}T_{12}(1) + M_{j3}T_{22}(1)) \\
&\qquad - T_{12}(\zeta) \big] (\cdot) \\
&\mathfrak{R}_2\mathfrak{B} = -v(1-R) \left[T_{33}(\zeta)(M_{32}T_{12}(1) + M_{33}T_{22}(1)) \right] (\cdot)
\end{aligned} \tag{13}$$

Since the system generator $\mathfrak{A}$ is not self-adjoint, the resolvent operator for the adjoint system shall also be obtained. This is done in a similar manner as the original system, resulting in a closed-form expression for the adjoint resolvent operator $\mathfrak{R}^*(s,\mathfrak{A}^*)$. To avoid redundancy, the derivation of the resolvent operator for the adjoint system is not included in this manuscript.

D. Cayley-Tustin time discretization

To implement the system on digital controllers, it is necessary to transition to a discrete-time framework while preserving critical properties such as stability and controllability. The Cayley-Tustin time-discretization method achieves this by mapping the continuous-time system to the discrete domain [19], [20]. This Crank-Nicolson type of discretization is also known as the lowest order symplectic integrator in Gauss quadrature-based Runge-Kutta methods [21]. Considering Δt as the sampling time, and assuming a piecewise constant input within time intervals (zero-order hold), the discrete-time representation $\underline{x}(\zeta,k) = \mathfrak{A}_d\underline{x}(\zeta,k-1) + \mathfrak{B}_d u(k)$ is obtained, with discrete-time operators $\mathfrak{A}_d$ and $\mathfrak{B}_d$ defined in (14), where $\alpha = 2/\Delta t$.

$$\begin{bmatrix} \mathfrak{A}_d & \mathfrak{B}_d \end{bmatrix} = \begin{bmatrix} -I + 2\alpha\mathfrak{R}(\alpha,\mathfrak{A}) & \sqrt{2\alpha}\mathfrak{R}(\alpha,\mathfrak{A})\mathfrak{B} \end{bmatrix} \tag{14}$$

As required for systems with nonself-adjoint generators, the adjoint discrete-time operators $\mathfrak{A}_d^*$ and $\mathfrak{B}_d^*$ are also obtained in a similar manner, as shown in (15).

$$\begin{bmatrix} \mathfrak{A}_d^* & \mathfrak{B}_d^* \end{bmatrix} = \begin{bmatrix} -I + 2\alpha\mathfrak{R}^*(\alpha,\mathfrak{A}^*) & \sqrt{2\alpha}\mathfrak{B}^*\mathfrak{R}^*(\alpha,\mathfrak{A}^*) \end{bmatrix} \tag{15}$$

E. Model predictive control design

The proposed MPC, as shown in Fig. 3, is developed in this section with the goal of stabilizing the given unstable infinite-dimensional system within an optimal framework while satisfying input constraints. An infinite-time open-loop objective function sets the foundation of the controller design in the discrete-time setting at each sampling instant k, which consists of a weighted sum of state deviations and actuation costs for all future time instances, subject to the system dynamics and input constraints, as shown in (16).

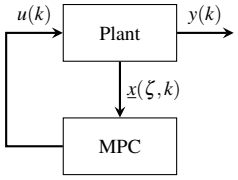

Fig. 3. Proposed full-state feedback model predictive control system.

$$\begin{aligned}
\min_{U} \quad & \sum_{l=0}^{\infty} \langle \underline{x}(\zeta,k+l|k), \mathfrak{Q}\underline{x}(\zeta,k+l|k) \rangle \\
& + \langle u(k+l+1|k), \mathfrak{F}u(k+l+1|k) \rangle \\
\text{s.t.} \quad & \underline{x}(\zeta,k+l|k) = \mathfrak{A}_d\underline{x}(\zeta,k+l-1|k) + \mathfrak{B}_d u(k+l|k) \\
& u^{min} \le u(k+l|k) \le u^{max}
\end{aligned} \tag{16}$$

where $\mathfrak{Q}$ and $\mathfrak{F}$ are positive definite operators of appropriate dimensions, responsible for penalizing state deviations and actuation costs, respectively. The notation $(k+l|k)$ indicates the future time states or input instance $k+l$ obtained at time k. The infinite-time optimization problem may be reduced to a finite-time setup by assigning zero-input beyond

a certain control horizon N, resulting in the optimization problem in (17).

$$\begin{aligned}\min_{U} \quad & \sum_{l=0}^{N-1} \langle \underline{x}(\zeta,k+l|k), \mathfrak{Q}\underline{x}(\zeta,k+l|k)\rangle \\ & +\langle u(k+l+1|k), \mathfrak{F}u(k+l+1|k)\rangle \\ & +\langle \underline{x}(\zeta,k+N|k), \mathfrak{P}\underline{x}(\zeta,k+N|k)\rangle \\ \text{s.t.} \quad & \underline{x}(\zeta,k+l|k) = \mathfrak{A}_d\underline{x}(\zeta,k+l-1|k) + \mathfrak{B}_d u(k+l|k) \\ & u^{min} \le u(k+l|k) \le u^{max} \\ & \langle \underline{x}(\zeta,k+N|k), \underline{\phi_u}(\zeta)\rangle = 0 \end{aligned} \tag{17}$$

Obtained as the solution to the discrete-time Lyapunov equation, $\mathfrak{P}$ is the terminal cost operator as shown in (18); which can be proven to be positive definite only if the terminal state $\underline{x}(\zeta,k+N|k)$ is in a stable subspace. Therefore, an equality constraint is introduced to guarantee that the resulting quadratic optimization problem is convex. The terminal constraint is enforced by setting the projection of the terminal state onto the unstable subspace of the system to zero [9], [10], [20]. Here, $\underline{\phi_u}(\zeta)$ is the set of unstable eigenfunctions of the system, for all eigenvalues where $\mathrm{Re}(\lambda_u) \ge 0$.

$$\mathfrak{P}(\cdot) = \sum_{m=0}^{\infty}\sum_{n=0}^{\infty} -\frac{\langle \underline{\phi_m}, \mathfrak{Q}\underline{\psi_n}\rangle}{\lambda_m + \overline{\lambda_n}} \langle (\cdot), \underline{\psi_n}\rangle \phi_m \tag{18}$$

One may further process the optimization problem in (17) to obtain a standard format for quadratic programming (QP) solvers by substituting the future states in terms of the current state and the sequence of future inputs using system dynamics expression. The resulting QP problem is given in (19). The optimal input sequence U is then obtained by solving the QP problem at each sampling instant k. To implement a receding horizon control strategy, only the first input of the optimal sequence $u(k+1|k)$ is applied to the system, and the optimization problem is solved again at the next sampling instant $k+1$.

$$\begin{aligned} \min_{U} & J = U^T\langle I,H\rangle U + 2U^T\langle I, P\underline{x}(\zeta,k|k)\rangle \\ \text{s.t.} \quad & U^{min} \le U \le U^{max} \\ & T_u\underline{x}(\zeta,k|k) + S_u U = 0 \end{aligned}$$

with $H =$

$$\begin{bmatrix} \mathfrak{B}_d^*\mathfrak{P}\mathfrak{B}_d + \mathfrak{F} & \mathfrak{B}_d^*\mathfrak{A}_d^*\mathfrak{P}\mathfrak{B}_d & \cdots & \mathfrak{B}_d^*\mathfrak{A}_d^{*N-1}\mathfrak{P}\mathfrak{B}_d \\ \mathfrak{B}_d^*\mathfrak{P}\mathfrak{A}_d\mathfrak{B}_d & \mathfrak{B}_d^*\mathfrak{P}\mathfrak{B}_d + \mathfrak{F} & \cdots & \mathfrak{B}_d^*\mathfrak{A}_d^{*N-2}\mathfrak{P}\mathfrak{B}_d \\ \vdots & \vdots & \ddots & \vdots \\ \mathfrak{B}_d^*\mathfrak{P}\mathfrak{A}_d{}^{N-1}\mathfrak{B}_d & \mathfrak{B}_d^*\mathfrak{P}\mathfrak{A}_d{}^{N-2}\mathfrak{B}_d & \cdots & \mathfrak{B}_d^*\mathfrak{P}\mathfrak{B}_d + \mathfrak{F} \end{bmatrix}$$

$$\begin{aligned} P &= \begin{bmatrix} \mathfrak{B}_d^*\mathfrak{P}\mathfrak{A}_d & \mathfrak{B}_d^*\mathfrak{P}\mathfrak{A}_d{}^2 & \dots & \mathfrak{B}_d^*\mathfrak{P}\mathfrak{A}_d{}^N \end{bmatrix}^T \\ T_u(\cdot) &= \begin{bmatrix} \langle \mathfrak{A}_d{}^N(\cdot), \underline{\phi_u}\rangle \end{bmatrix} \\ S_u &= \begin{bmatrix} \langle \mathfrak{A}_d{}^{N-1}\mathfrak{B}_d, \underline{\phi_u}\rangle & \langle \mathfrak{A}_d{}^{N-2}\mathfrak{B}_d, \underline{\phi_u}\rangle & \dots & \langle \mathfrak{B}_d, \underline{\phi_u}\rangle \end{bmatrix} \\ U &= \begin{bmatrix} u(k+1|k) & u(k+2|k) & \dots & u(k+N|k) \end{bmatrix}^T \end{aligned} \tag{19}$$

III. Results and Discussion

Numerical simulations for the open-loop system and the closed-loop system under the proposed MPC are presented in this section, with parameters chosen according to Table I. As the eigenvalue distribution obtained in Fig(2) suggests, the open-loop system is unstable due to the presence of an eigenvalue with positive real part. The zero-input response of the system is shown in Fig(4) where the initial condition for the reactor is set to $c(\zeta,0) = \sin^2(\pi\zeta)$. The recycle stream is assumed to be empty at the beginning of the simulation.

An infinite-dimensional MPC is designed and applied to the unstable system. The state deviation and actuation penalty terms are set as $\mathfrak{Q} = 0.04I$ and $\mathfrak{F} = 27$. The sampling time and the horizon length for the MPC are set to $\Delta t = 20$ s and $N = 9$, respectively. Lastly, the input constraints are assumed to be $0 \le u(t) \le 0.15$. The closed-loop response of the system is shown in Fig(5) and the control input as well as the system output is shown in Fig(6). It may be confirmed that the MPC successfully stabilizes the unstable system while satisfying the input constraints.

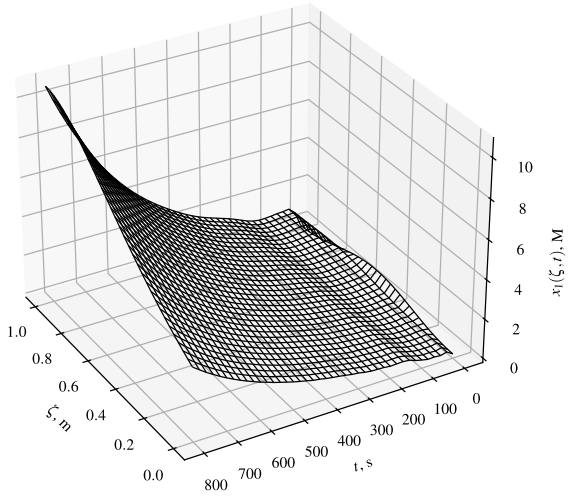

Fig. 4. Open-loop concentration profile along the reactor.

One interesting aspect of considering recycle stream is the oscillatory behavior of the system dynamics. While axial dispersion reactors show no oscillation in the absence of recycle, the nature of recycle streams can introduce such behavior. The choice of control horizon is another key factor. A short control horizon relative to the resident time of the recycle stream can lead to oscillatory input profiles due to the presence of delayed recycle stream. In this example, the control horizon, i.e. 180 s, is set to be considerably longer than the recycle delay, which is 80 s; resulting in a non-oscillatory input profile.

IV. Conclusion

In this work, model predictive control of an axial dispersion tubular reactor equipped with recycle is addressed,

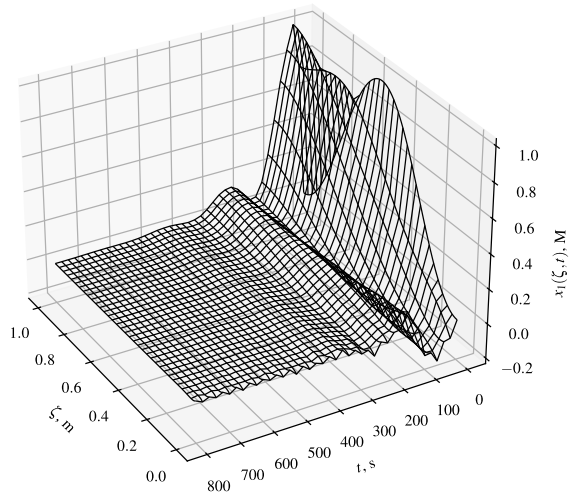

Fig. 5. Stabilized reactor concentration profile under the proposed MPC.

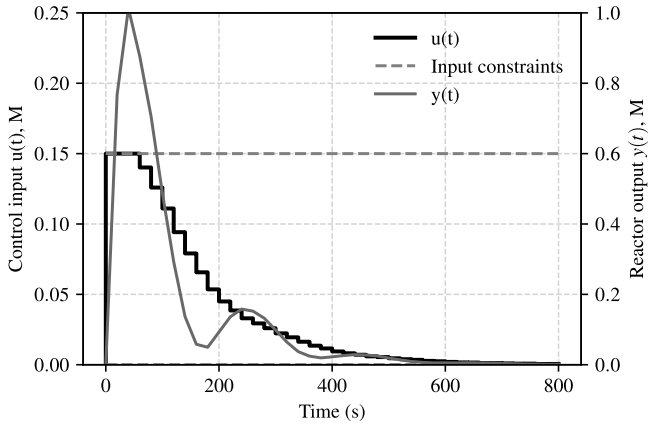

Fig. 6. Input constraints, the obtained input profile, and the reactor output under the proposed MPC.

while considering the delay imposed by the recycle stream. This setup is common in industry but has received limited attention in the chemical engineering distributed parameter systems literature. The diffusion-convection-reaction dynamics of the reactor is modeled by a second-order parabolic PDE, while a notion of state delay is introduced to account for the delay imposed by the recycle stream. The state delay is addressed as a separate transport PDE, resulting in a boundary-controlled system governed by a coupled set of parabolic and hyperbolic PDEs under Danckwerts boundary conditions. Utilizing late-lumping approach, the resolvent operator is obtained in a closed form in order to preserve the infinite-dimensional nature of the system without requiring spatial discretization. To implement MPC as a digital controller, the Cayley-Tustin transformation is used. This Crank-Nicolson type of discretization is chosen as it maintains important properties of the system such as stability and controllability when mapping the continuous-time system to a discrete-time one. Numerical simulations demonstrate the effectiveness of the proposed controller in stabilizing an unstable system while satisfying input constraints. The proposed approach can be extended further to include state reconstruction to establish an output-feedback controller. Addressing disturbance rejection or set-point tracking, as well as considering the effects of temperature may also be considered in future works.

REFERENCES

[1] W. H. Ray, *Advanced process control*. McGraw-Hill: New York, NY, USA, 1981.

[2] E. Davison, "The robust control of a servomechanism problem for linear time-invariant multivariable systems," *IEEE transactions on Automatic Control*, vol. 21, no. 1, pp. 25–34, 1976.

[3] A. A. Moghadam, I. Aksikas, S. Dubljevic, and J. F. Forbes, "Infinite-dimensional lq optimal control of a dimethyl ether (dme) catalytic distillation column," *Journal of Process Control*, vol. 22, no. 9, pp. 1655–1669, 2012.

[4] P. D. Christofides and P. Daoutidis, "Feedback control of hyperbolic pde systems," *AIChE Journal*, vol. 42, no. 11, pp. 3063–3086, 1996.

[5] M. Krstic and A. Smyshlyaev, "Backstepping boundary control for first-order hyperbolic pdes and application to systems with actuator and sensor delays," *Systems & Control Letters*, vol. 57, no. 9, pp. 750–758, 2008.

[6] X. Xu and S. Dubljevic, "The state feedback servo-regulator for countercurrent heat-exchanger system modelled by system of hyperbolic pdes," *European Journal of Control*, vol. 29, pp. 51–61, 2016.

[7] P. D. Christofides, "Robust control of parabolic pde systems," *Chemical Engineering Science*, vol. 53, no. 16, pp. 2949–2965, 1998.

[8] S. Dubljevic, N. H. El-Farra, P. Mhaskar, and P. D. Christofides, "Predictive control of parabolic pdes with state and control constraints," *International Journal of Robust and Nonlinear Control: IFAC-Affiliated Journal*, vol. 16, no. 16, pp. 749–772, 2006.

[9] S. Khatibi, G. O. Cassol, and S. Dubljevic, "Model predictive control of a non-isothermal axial dispersion tubular reactor with recycle," *Computers & Chemical Engineering*, vol. 145, p. 107159, 2021.

[10] R. Curtain and H. Zwart, *Introduction to infinite-dimensional systems theory: a state-space approach*. Springer Nature, 2020, vol. 71, ch. 3.2: 'Riesz-spectral operators', pp. 79–108.

[11] M. Krstić, *Delay compensation for nonlinear, adaptive, and PDE systems*, ser. Systems & control. Birkhäuser, 2009, ch. 1.8: 'DDE or Transport PDE Representation', p. 9.

[12] S. Hiratsuka and A. Ichikawa, "Optimal control of systems with transportation lags," *IEEE Transactions on Automatic Control*, vol. 14, no. 3, pp. 237–247, 1969.

[13] L. Mohammadi, I. Aksikas, S. Dubljevic, and J. F. Forbes, "Lq-boundary control of a diffusion-convection-reaction system," *International Journal of Control*, vol. 85, no. 2, pp. 171–181, 2012.

[14] G. O. Cassol and S. Dubljevic, "Discrete output regulator design for a mono-tubular reactor with recycle," in *2019 American Control Conference (ACC)*, 2019, pp. 1262–1267.

[15] G. Ozorio Cassol, D. Ni, and S. Dubljevic, "Heat exchanger system boundary regulation," *AIChE Journal*, vol. 65, no. 8, p. e16623, 2019.

[16] J. Qi, S. Dubljevic, and W. Kong, "Output feedback compensation to state and measurement delays for a first-order hyperbolic pide with recycle," *Automatica*, vol. 128, p. 109565, 2021.

[17] O. Levenspiel, *Chemical reaction engineering*. John wiley & sons, 1998.

[18] P. V. Danckwerts, "Continuous flow systems. distribution of residence times," *Chemical engineering science*, vol. 50, no. 24, pp. 3857–3866, 1993.

[19] V. Havu and J. Malinen, "The cayley transform as a time discretization scheme," *Numerical Functional Analysis and Optimization*, vol. 28, no. 7-8, pp. 825–851, 2007.

[20] Q. Xu and S. Dubljevic, "Linear model predictive control for transport-reaction processes," *AIChE Journal*, vol. 63, no. 7, pp. 2644–2659, 2017.

[21] E. Hairer, M. Hochbruck, A. Iserles, and C. Lubich, "Geometric numerical integration," *Oberwolfach Reports*, vol. 3, no. 1, pp. 805–882, 2006.